Ice lithography for 3D nanofabrication

Zhao, Ding; Han, Anpan; Qiu, Min

Published in:
Science Bulletin

Link to article, DOI:
10.1016/j.scib.2019.06.001

Publication date:
2019

Document Version
Publisher's PDF, also known as Version of record

Science Bulletin 64 (2019) 865–871

Contents lists available at ScienceDirect

Science Bulletin

journal homepage: www.elsevier.com/locate/scib

Progress

Ice lithography for 3D nanofabrication

Ding Zhao [a], Anpan Han [b], Min Qiu [c,d,*]

[a] National Centre for Nano Fabrication and Characterization, Technical University of Denmark, Kongens Lyngby, 2800, Denmark
[b] Department of Mechanical Engineering, Technical University of Denmark, Kongens Lyngby, 2800, Denmark
[c] Key Laboratory of 3D Micro/Nano Fabrication and Characterization of Zhejiang Province, School of Engineering, Westlake University, Hangzhou 310024, China
[d] Institute of Advanced Technology, Westlake Institute for Advanced Study, Hangzhou 310024, China

ARTICLE INFO

Article history:
Received 8 April 2019
Received in revised form 14 May 2019
Accepted 30 May 2019
Available online 3 June 2019

Keywords:
Nanotechnology
Nanofabrication
Electron-beam lithography
Ice lithography
3D nanofabrication
Additive manufacturing
Organic ice

ABSTRACT

Nanotechnology and nanoscience are enabled by nanofabrication. Electron-beam lithography, which makes 2D patterns down to a few nanometers, is one of the fundamental pillars of nanofabrication. Recently, significant progress in 3D electron-beam-based nanofabrication has been made, such as the emerging ice lithography technology, in which ice thin-films are patterned by a focused electron-beam. Here, we review the history and progress of ice lithography, and focus on its applications in efficient 3D nanofabrication and additive manufacturing or nanoscale 3D printing. The finest linewidth made using frozen octane is below 5 nm, and nanostructures can be fabricated in selected areas on non-planar surfaces such as freely suspended nanotubes or nanowires. As developing custom instruments is required to advance this emerging technology, we discuss the evolution of ice lithography instruments and highlight major instrumentation advances. Finally, we present the perspectives of 3D printing of functional materials using organic ices. We believe that we barely scratched the surface of this new and exciting research area, and we hope that this review will stimulate cutting-edge and interdisciplinary research that exploits the undiscovered potentials of ice lithography for 3D photonics, electronics and 3D nanodevices for biology and medicine.

1. Introduction

Nanotechnology has a revolutionary impact in the twenty-first century. Nanofabrication technologies are instruments and methods that e.g. position, fabricate and interconnect structures at the nanometer scale. Miniaturization and integration are the core of nanofabrication technology. Examples are the lithography and plasma etching methods for shrinking transistors down to 10 nm. Nanofabrication is also a key enabling technology for promising emerging nanostructures and materials, and examples are nanoparticles, nanowires, metamaterials, and two-dimensional materials, which are finding applications in energy [1], electronics [2], chemical engineering [3], biomedicine [4], and quantum technology [5]. State-of-the-art nanofabrication is a 2D technology, such nanodevices are made on the surface of substrates, and the bulk material is unused. In other words, only a tiny fraction of the available functional material is used to make functional devices. To take advantage of the bulk material and obtain highly integrated devices motivate the development of advanced nanotechnologies for three-dimensional (3D) nanofabrication.

Being one of the most important nanofabrication methods, electron-beam lithography (EBL) produces patterns down to a few nanometers [6]. The EBL process contains three steps. First, a resist material is applied on a sample with a mirror-polished flat surface by spin or spray coating. Second, a nanometer-size focused beam of electrons exposes a designed pattern in the resist, which locally changes the chemical character of the resist. Third, the sample is immersed into a solvent for resist development. This process removes the exposed area for a positive-tone resist or unexposed area for a negative-tone resist, and after drying, resist patterns remain on the substrate. By employing an aberration-corrected scanning transmission electron microscope (STEM), EBL can achieve single digit nanometer length scale [7,8]. Since spin and spray coating can only attain uniform thin resist coatings on planar substrates, EBL processing is limited to flat substrates. For EBL on non-flat surfaces, polystyrene resists can be applied by thermal evaporation. For example, EBL has been implemented on an atomic force microscope (AFM) cantilever and optical fibers [9].

Focused electron beam induced deposition (FEBID) is a nanoscale additive nanomanufacturing technique, which enables direct-write synthesis of 3D architectures on complex sample topographies [10,11]. In FEBID, injected gas molecules are absorbed onto the sample surface and then dissociated by incident

* Corresponding author.
E-mail address: qiu_lab@westlake.edu.cn (M. Qiu).

https://doi.org/10.1016/j.scib.2019.06.001
2095-9273/

energetic electrons, leading to the formation of a solid deposit. Because of its working principle, the FEBID process speed is slower than that of EBL. Nevertheless, a dramatic development in FEBID is the creation of a free-standing truncated icosahedron with the characteristic edge dimension down to 200 nm [12], which is unachievable by EBL.

Invented in 2005, ice lithography (IL) is a versatile technique, and it has shown great potential in fabrication of 3D nanostructures. In this review, current status and future perspectives of IL are presented. Furthermore, it also covers different ice resists and IL instrument design. Special emphasis is placed on advantages of IL for 3D nanofabrication.

It is important to point out that IL is a nanolithography tool, and for many applications, EBL and FEBID are more suited than IL. For instance, FEBID is a more powerful method for building extremely small 3D nanostructures. For 2D patterning on larger samples, EBL resists can be applied uniformly by spin coating, and EBL provides faster patterning speed than IL. In EBL, an additional conductive layer such as an Al thin-film can be applied on the top of thick resist layer to relieve undesired charging effects, and Al can be removed before resist development. However, this strategy is not applicable to IL, since a metal film covering on water ice will affect the further patterning process.

2. Ice lithography method and performance

The Nanopore group at Harvard University first proposed ice lithography [13]. The basic principle of ice lithography is simple. Provided by a gas injection system (GIS) inside an electron microscope, a precursor gas condenses on a cold surface is exposed by a focused electron beam. This brief description shows similarity to FEBID. A closer look at the process flow of IL in Fig. 1, however, reveals that IL is an electron-solid-surface interaction while FEBID is an electron-gas-surface interaction. During IL, vaporized material firstly condenses onto the precooled sample (130 K) and forms a uniform amorphous ice thin-film. Then the e-beam exposes the ice layer to generate nanoscale patterns. This is a subtractive patterning process for water ice, where ice within exposure areas vanishes (Fig. 1b and c). The mechanism is yet unclear, but probably due to electron-stimulated reactions at solid water [14,15]. Final pattern transfer is realized through metallization. All above IL processes are accomplished in one instrument except the last lift-off step or "melt-off" step. For alkane ice, cross-linking occurs during electron-ice interaction. Only heavily cross-linked molecules within the exposure area are solidified and remain after heating the sample, acting as an additive process (Fig. 1f and g). The carbonaceous products are nonvolatile and very stable at ambient conditions. They can be used as masks for plasma etching of the underlying material [16].

Ice lithography research is still in its infancy, and only a few carefully selected ice materials have been studied. Currently, only water ice is capable of acting as a positive-tone lithography resist, and it has been used to fabricate nanostructures with sub-10 nm features (Fig. 2a). Organic ice from simple organic molecules, e.g. alcohols, alkane, demonstrates negative-resist-like capabilities. Fig. 2b shows 100-nm-wide and 60-nm-wide lines patterned in nonane and anisole ice, respectively. The linewidth of patterns made in organic ice resist could be significantly reduced to less than 5 nm (Fig. 2c) using an electron beam provided by a transmission electron microscope (TEM) [19], which is comparable with the smallest features made in EBL resists [8]. These sub 5-nm lines were patterned on 10-nm-thick frozen octane [19]. The e-beam energy is 80 keV, and the dose is 11 nC/cm. As illustrated in Fig. 2f, linewidth depends both on beam current and molecular length of the ice resist.

Apart from the linewidth, contrast and sensitivity are also important resist properties. The plots shown in Fig. 2d and e show the contrast curves for positive-tone water ice resist and negative-tone nonane ice resist. The thickness of ice resist is proportional to the pressure drop in the GIS. For water ice, it can be measured in situ through tilted SEM imaging. For organic ice, it is challenging to measure the initial ice thickness, and we obtain the thickness of exposed resist by AFM. Electron dose is the number of electrons that are applied to a unit area of resists, and it is related to patterning speed. Contrast is the slope of the curve, expressed by $\gamma = 1/\log_{10}(D_{100}/D_0)$. D_0 is the maximum electron dose at which the resist is not yet affected by e-beam exposure. D_{100}, also called critical dose, is the minimum electron dose needed for complete exposure of the resist. D_{50} is the dose at which the exposed features have half of the thickness of the original positive-tone resist or of a fully-exposed negative-tone resist. Here, we summarize and compare IL resists with EBL resists and a FEBID precursor in Table 1. FEBID requires 250 mC/cm^2 to deposit a single atomic layer from an organometallic precursor, and this dose is comparable with the critical dose for water ice resist. In FEBID, the incident electrons must interact with the surface-adsorbed gas molecules to form a solid monolayer, and more electrons are needed for thicker deposits. Therefore, the FEBID critical dose increases in proportion to the thickness of deposit. But in IL, the gas molecules are frozen into a solid thin-film, and the energetic primary electrons penetrate the entire ice film, then the secondary electrons play a major role in the cross-linking of organic molecules [19]. Compared to FEBID,

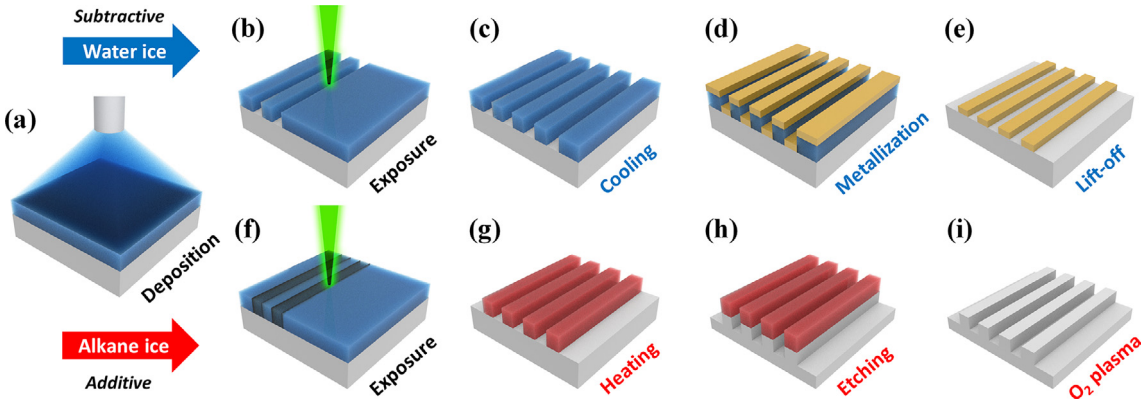

Fig. 1. (Color online) IL Process flow. (a) Vaporized material is frozen onto the cold sample to form a layer of ice resist. (b and f) Focused e-beam exposes ice resist for patterning. For water ice, (c) the exposed ice vanishes and pattern transfer is realized after (d) metallization and (e) lift-off. For alkane ice, (g) only the exposed areas remain after heating and pattern transfer done by (h) plasma etching and (i) oxygen plasma for resist removal.

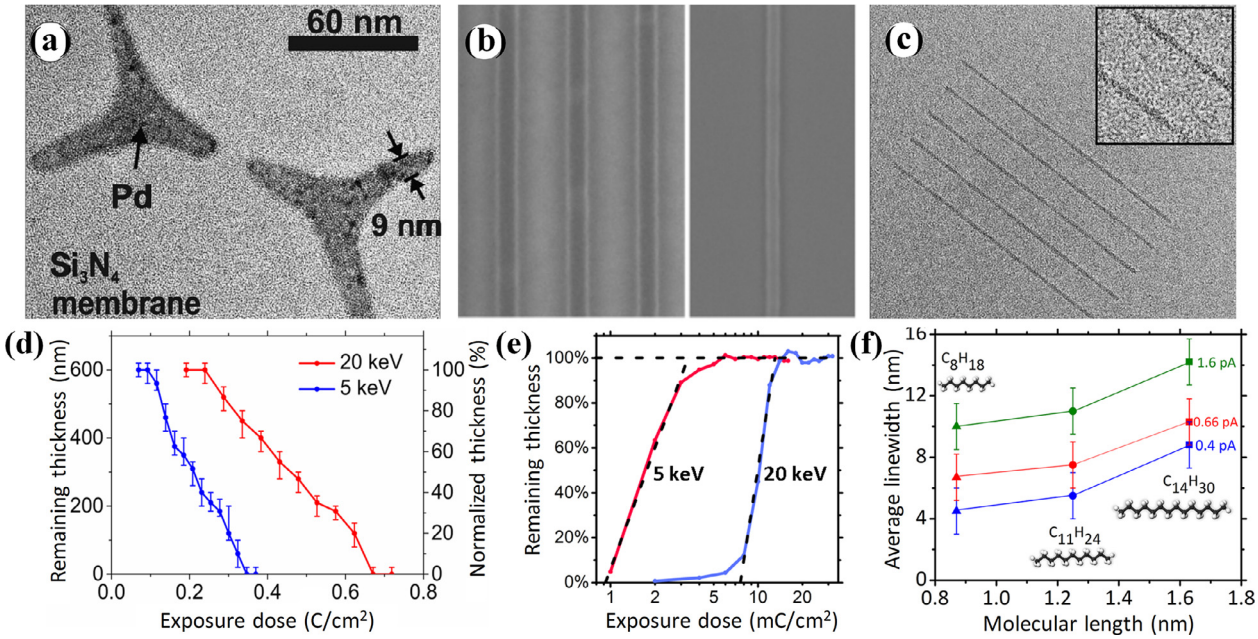

Fig. 2. (Color online) Minimal pattern size and contrast curves of ice resists. (a) TEM image of three-bladed Pd pattern made by IL with water ice, and the minimal feature size is less than 9 nm. (b) SEM images of 100-nm-wide (left panel) and 60-nm-wide (right panel) lines patterned using nonane and anisole ice, respectively. (c) The smallest linewidth of 4.5 nm is patterned on frozen octane using an electron beam provided by a TEM. (d) Contrast curves with error bars for water ice. (e) Contrast curves for nonane ice. (f) Linewidth of the patterned structure depends on the TEM electron beam current (proportional to electron dose) and molecular length of ice resist. Figure reproduced with permission: (a) Ref. [17], Copyright 2012 American Chemical Society (ACS); (b) Ref. [18], Copyright 2017 ACS; (c, f) Ref. [19], Copyright 2018 ACS; (d) Ref. [20], Copyright 2018 ACS; (e) Ref. [21], Copyright 2018 Elsevier.

Table 1
Contrast and sensitivity of ice resists compared with EBL resists and a FEBID precursor. The total dose (equivalent to D_{100}) for FEBID depositing a single atomic layer denoted with asterisk.

Method	Resist/Precursor	Tone	Electron energy (keV)	Contrast γ	Sensitivity (D_{50}, mC/cm^2)	Reference
IL	H_2O	Positive	5, 20	1.84, 2.24	200, 450	[20]
	C_7H_8O	Negative	5, 20	0.91, 1.03	3, 15	[22]
	C_8H_{18}	Negative	80	1.62	40	[19]
	C_9H_{20}	Negative	5, 20	1.8, 4.3	2, 10	[21]
	$C_{11}H_{24}$	Negative	80	1.43	20	[19]
	$C_{14}H_{30}$	Negative	80	0.18	20	[19]
EBL	PMMA	Positive	50	5.4	0.42	[23]
	HSQ	Negative	70	5	0.15	[24]
FEBID	$MeCpPtMe_3$	Negative	20	–	250*	[25]

the critical dose in IL is less dependent on resist thickness. Moreover, the critical dose for nonane ice is two orders of magnitude smaller than water ice. Hence, it is much faster to process organic ices and allows larger patterns.

3. Toward 3D nanofabrication

3.1. Fabrication on non-flat surfaces

Interest for fabrication on non-flat surfaces is growing in different fields such as micro- and nano-optics, MEMS, and biophotonics. For example, in optics, an aplanatic lens with aberration correction consists of at least two elements, while optical metasurfaces can manipulate light at the subwavelength scale and exhibit aberration correction function using a single element. However, the fabrication of an aplanatic metasurface is challenging, because one necessary step is to pattern nanostructures on a curved surface [26]. Another example is the realization of miniature optical instruments such as endoscopes and fiber-imaging systems, which also relies on advanced 3D nanofabrication techniques [27].

The first advantage of IL is to process samples with non-flat and irregular surfaces. Different from spin coating of EBL resists, ice resists are able to coat all accessible freezing surfaces of the sample during ice deposition [17]. This is nicely illustrated by patterning on AFM probes. First, a well-controlled water vapor condenses on a pyramidal tip of an AFM probe. Second, water ice then is removed by patterning a rectangle area centered on the tip by the focused e-beam, which reveals the underlying tip. Third, with in-situ metal deposition, Au with Ti adhesive layer covers the entire probe including the exposed tip. Finally, after immersing the sample in isopropanol and melting water ice at room temperature, the pyramidal surface is clean and residual-free, and only a Ti/Au cap remains on the AFM apex (Fig. 3a inset).

The second advantage of IL is the ability to pattern on a tiny and fragile nanostructure, exemplified in the case of suspended single-walled carbon nanotubes (SWCNT). It is very interesting and also extremely challenging. Here, the suspended carbon nanotubes were grown over a trench in a very thin and fragile free-standing silicon nitride membrane [17] (Fig. 3b inset). Spin and spray coating of EBL resists can not apply a uniform layer of resist onto such suspended nanotubes, and the surface tension during resist drying

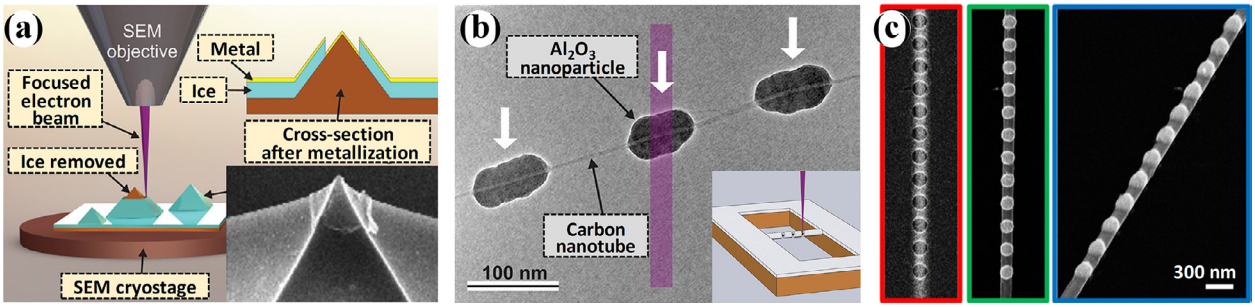

Fig. 3. (Color online) IL on non-planar surfaces. (a) Only the tip area of an AFM probe is capped with 1 nm Ti and 20 nm Au. (b) Al_2O_3 nanoparticles grown by ALD on carbon nanotubes, where Ti seeds have been fabricated previously through IL. The white arrows indicate the locations where ice is removed. (c) Metallic nanoparticle arrays on a single Ag nanowire with a diameter of 160 nm. SEM images with red and green frames show the nanowire after e-beam exposure and metallization, respectively. Figure reproduced with permission: (a and b) Ref. [17], Copyright 2012 ACS; (c) Ref. [20], Copyright 2018 ACS.

will destroy the nanostructure. However, water ice resist can condense on cold carbon nanotubes. After e-beam removal of the ice, Ti is deposited onto the surface of the nanotube as a seed layer for Al_2O_3 growth by atomic layer deposition (ALD). The IL patterning combined with ALD processing can precisely control the locations and sizes of the Al_2O_3 particles.

For the third advantage, we are able to observe nanostructures under the ice resist through SEM imaging, benefiting from the very low sensitivity of water ice. It is not possible with a sensitive EBL resist, as SEM imaging would expose the resist. This advantage is illustrated in Fig. 3c by patterning on a single nanowire, whereupon we can align nanoparticles neatly [20]. The diameter of the nanowire is 160 nm, and the alignment accuracy is less than 50 nm.

3.2. Nanoscale additive manufacturing

Additive manufacturing (AM), also known as 3D printing or rapid prototyping, refers to a class of manufacturing processes, which enables unprecedented engineering and production possibilities. In AM, a part is built by adding layers of material on top of one another, and AM objects are fabricated from metals, ceramics and opaque plastics. Examples of AM methods are inkjet printing [28], stereolithography [29], two-photon polymerization [30], and FEBID. For EBL, patterning related to premade nanostructures is usually obtained through overlay process. Such a stacking layer strategy can also be regarded as an AM processing, where the fabrication of each layer needs a series of procedures including spin-coating, lithography, developing, deposition and lift-off. Here, additional markers should be fabricated previously around the exposure area for registration and alignment between layers. However, none of these technologies is able to deliver AM on the nanoscale with competitive throughput, and achieve a balance among resolution, alignment, stability, and adaptability.

Ice lithography with water ice enables marker-less fabrication, which results in much fewer processing steps required for fabricating 3D nanostructures [20]. Fig. 4 shows fabrication of a pyramidal nanostructure by repeating ice deposition, e-beam exposure and metallization three times. Here, 10 processing steps and one load-unload operation on the instrument are required. In comparison, the EBL procedure for fabricating such a structure includes 19 processing steps and 8 load-unload operations. IL can also implement similar architecture with organic ice (Fig. 4k) through the cycle of deposition and exposure [18]. Moreover, applying the strategy of greyscale lithography, IL with water ice successfully fabricates partially suspended nanostructures like a mushroom (Fig. 4l) or a bridge (Fig. 4m). This flexible approach combined with layer-stacking strategy brings new and exciting opportunities in 3D nanofabrication.

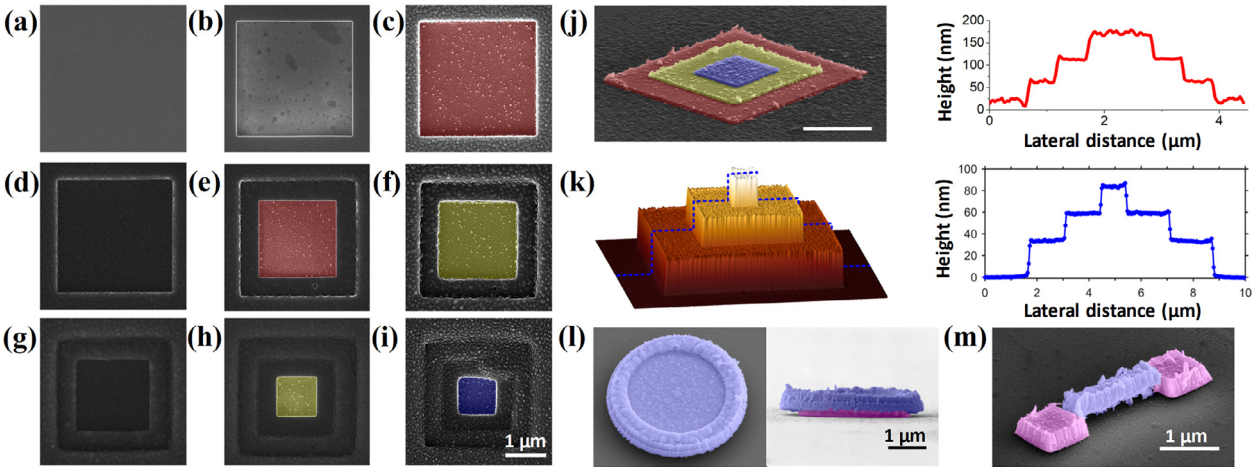

Fig. 4. (Color online) 3D layered and suspended nanostructures produced by IL. In-situ SEM images after different processing steps including ice deposition (a, d, and g), e-beam exposure (b, e, and h) and metallization (c, f, and i). A pyramidal nanostructure obtained using water ice (j) or organic ice (k), with corresponding line scan by AFM. Similar to greyscale lithography, IL can also realize 3D mushroom-like (l) and bridge-like (m) nanostructures. Figure reproduced with permission: (a-j, l, and m) Ref. [20], Copyright 2018 ACS; (k) Ref. [18], Copyright 2017 ACS.

4. IL instrument and its evolution

Cutting-edge instrument research and development is the fundament of ice lithography research. Depending on the type of ice resists, an IL instrument consists of 5 or 6 subsystems (Fig. 5a). Subsystems 1 and 2 are off-the-shelf equipments, while the others are highly specialized.

1. The electron beam is provided by a scanning electron microscope (SEM).
2. An EBL module is needed for e-beam patterning.
3. A specially designed cryostage for sample cooling, and a cold trap to shield the sample from vacuum contaminants is required. A heater is fitted into the cryostage for the sublimation of organic ice.
4. Water or organic vapor is injected into the SEM chamber through a custom gas injection system, which also controls the deposition rate and final thickness of ice thin-films.
5. A load-lock allows fast sample transfer and exchange, while maintaining vacuum and cryogenic conditions in the process chamber.
6. For processing water ice, an additional integrated metallization system is necessary. In this metallization system, another cryostage is included to suppress the sublimation of water ice during thermal evaporation or magnetron sputtering of materials.

In 2005, the first report on nanopatterning ice with e-beam was carried out using a cryosystem designed for biological applications [13]. However, this instrument was ill-suited for IL. Five years later, in 2010, the same research group demonstrated the successful IL process for device fabrication, and the first dedicated IL instrument was reported [31].

Inspired and guided by the design and challenges of the original IL system, another two instruments have been constructed at Technical University of Denmark (DTU) [21] and Zhejiang University (ZJU) [20], respectively. The DTU design (Fig. 5b) is very accessible and modular. Only the load-lock is permanently installed on the SEM, while the other parts can be quickly removed, enabling flexible switching between an IL instrument and an SEM imaging system. Without a metallization system, the DTU IL instrument focuses on nanofabrication using organic ice resists. In contrast, the IL instrument in China (Fig. 5c) includes two metallization chambers. The small chamber is equipped with a "single-pot" evaporator, while the big ultrahigh vacuum (UHV) chamber with several metal sources allow high quality epitaxial thin-film deposition. Therefore, this instrument can also be used for in-situ characterization of thin-films growth at low temperature. To our best knowledge, the ZJU instrument is the most advanced instrument today. The research field is growing, and at least four other instruments around the world are under construction and development.

5. Opportunities and future perspectives

This review has shown that ice lithography appears highly promising for simplifying and streamlining fabrication and advancing 3D nanofabrication. We believe that there are many more unexplored opportunities in nanoscale additive manufacturing of functional materials. Using organic ices, the deposited

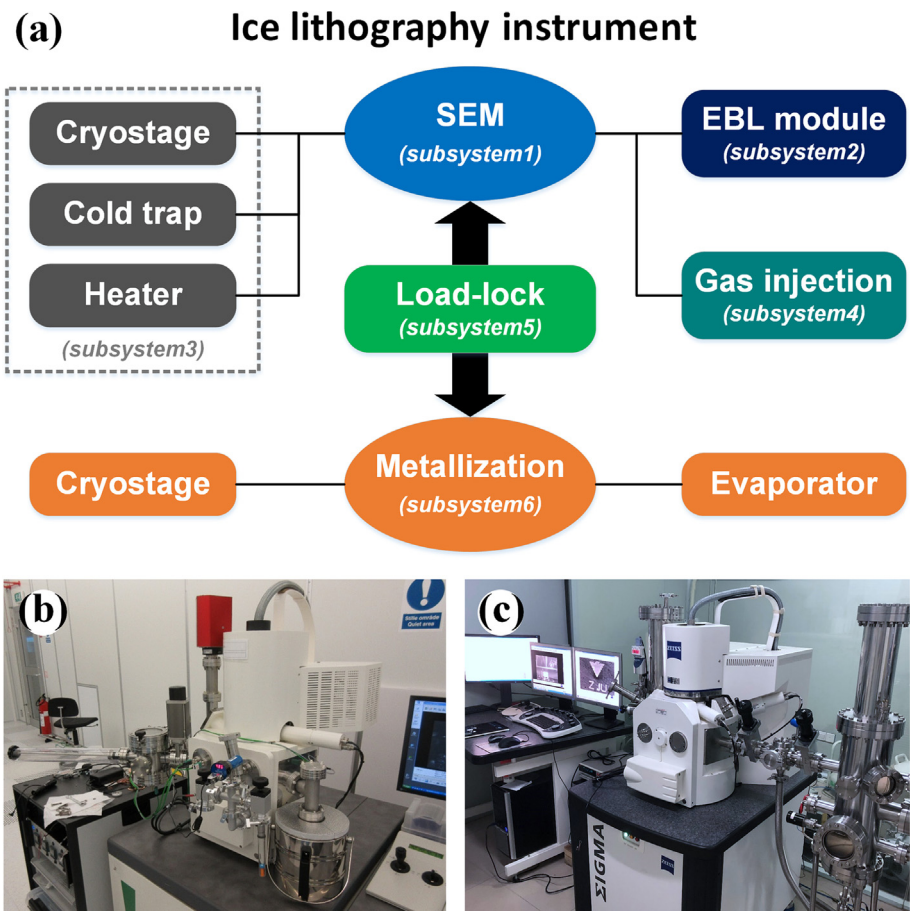

Fig. 5. (Color online) (a) IL instrument consisting of 5 (for organic ice) or 6 subsystems (for water ice). (b) IL instrument at Technical University of Denmark. (c) IL instrument at Zhejiang University.

material is a cross-linked product of the original organic ice. The resulting product shares common features with polymers of the original organic molecules. E.g. if alkane ices are used, the e-beam cross-linked product is chemically similar to cross-linked polythene. We hypothesize that polymer analogues with sufficient mechanical and dielectric properties can be additively fabricated by condensation of monomers and e-beam irradiation.

Apart from carbon and oxygen containing organic chemicals, organometallic compound that contains most elements of the periodic table is a very interesting class of organic chemicals. FEBID using organometallic precursors showed that pure gold (Au) [32] and superconducting tungsten (W) nanowires [33] can be formed. Using liquid phase precursors, FEBID can also deposit silver (Ag) and copper (Cu) structures [34], respectively. We hypothesize that metal can be additively made by freezing organometallic compounds, cross-linking by e-beam and post processing. This will pave the way for nanoscale 3D printing of nanophotonic and electronic devices.

Since organic semiconductor chemistry is also a branch of organic chemistry, we hypothesize that it is possible to condense and cross-link organic semiconductors. If IL is able to 3D print organic dielectrics, electric conductors, and semiconductors, it is likely that we could 3D print and do rapid prototyping of nanoelectronic devices. Hence, we propose the concept of *icetronics*.

Regarding to lithography perspectives, although this approach has many advantages, such as sub-10 nm resolution, easily doing lift-off and patterning on non-planar and fragile substrates, an essential issue is still not very clear: *why and how ice lithography works*. Both the underlying physics of electron-matter interactions and the science behind transforming ice into what it becomes after exposure need to be investigated in detail. Particularly, what else ice is effective as a positive-tone resist in IL, remains an open question. To investigate the principle of IL and approach its ultimate resolution will undoubtedly have major impact on 3D manufacturing.

For instrumentation perspectives, the current cryostage in IL instrument is cooled by liquid nitrogen, and its lowest temperature is around 130 K. More efficiently cooling is beneficial for exploring the ice resist with low freezing point, such as frozen CO_2, which has been applied to the dry lithography of organic semiconductors [35]. Moreover, none of the current IL instruments allows injection of two or more precursors and fast and automatic switching among them. In the future, a new prototype instrument equipped with more in-situ characterization techniques including a nanomanipulator for electrical measurement and nanoprofilometer for thickness measurement of ice thin-films, will provide more thorough understanding and more striking applications of IL. Finally, IL is a scalable technology, thanks to the development of multi-e-beam technologies with over 600,000 parallel e-beams [36]. High throughput production of 3D nanodevices is possible by combining IL and multi-e-beam technology.

Conflict of interest

The authors declare that they have no conflict of interest.

Acknowledgments

This work was supported by the National Key Research and Development Program of China (2017YFA0205700) and the National Natural Science Foundation of China (61425023). D.Z. acknowledges support from the European Union's Horizon 2020 research and innovation program under the Marie Skłodowska-Curie grant agreement No. 713683.

Author contributions

D.Z., A.H. and M.Q. discussed and prepared the review; all authors discussed and contributed to the final manuscript.

References

[1] Sun Y, Liu N, Cui Y. Promises and challenges of nanomaterials for lithium-based rechargeable batteries. Nat Energy 2016;1:16071.
[2] Orji NG, Badaroglu M, Barnes BM, et al. Metrology for the next generation of semiconductor devices. Nat Electron 2018;1:532–47.
[3] Yuan J, Liu X, Akbulut O, et al. Superwetting nanowire membranes for selective absorption. Nat Nanotechnol 2008;3:332–6.
[4] Shi J, Votruba AR, Farokhzad OC, et al. Nanotechnology in drug delivery and tissue engineering: from discovery to applications. Nano Lett 2010;10:3223–30.
[5] Ladd TD, Jelezko F, Laflamme R, et al. Quantum computers. Nature 2010;464:45–53.
[6] Chen Y. Nanofabrication by electron beam lithography and its applications: a review. Microelectron Eng 2015;135:57–72.
[7] Manfrinato VR, Zhang L, Su D, et al. Resolution limits of electron-beam lithography toward the atomic scale. Nano Lett 2013;13:1555–8.
[8] Manfrinato VR, Stein A, Zhang L, et al. Aberration-corrected electron beam lithography at the one nanometer length scale. Nano Lett 2017;17:4562–7.
[9] Zhang J, Con C, Cui B. Electron beam lithography on irregular surfaces using an evaporated resist. ACS Nano 2014;8:3483–9.
[10] Hagen CW. The future of focused electron beam-induced processing. Appl Phys A 2014;117:1599–605.
[11] Huth M, Porrati F, Dobrovolskiy OV. Focused electron beam induced deposition meets materials science. Microelectron Eng 2018;185–186:9–28.
[12] Fowlkes JD, Winkler R, Lewis BB, et al. Simulation-guided 3D nanomanufacturing via focused electron beam induced deposition. ACS Nano 2016;10:6163–72.
[13] King GM, Schürmann G, Branton D, et al. Nanometer patterning with ice. Nano Lett 2005;5:1157–60.
[14] Petrik NG, Kimmel GA. Electron-stimulated reactions at the interfaces of amorphous solid water films driven by long-range energy transfer from the bulk. Phys Rev Lett 2003;90.
[15] Petrik NG, Kavetsky AG, Kimmel GA. Electron-stimulated production of molecular oxygen in amorphous solid water. J Phys Chem B 2006;110:2723–31.
[16] Han A, Vlassarev D, Wang J, et al. Ice lithography for nanodevices. Nano Lett 2010;10:5056–9.
[17] Han A, Kuan A, Golovchenko J, et al. Nanopatterning on nonplanar and fragile substrates with ice resists. Nano Lett 2012;12:1018–21.
[18] Tiddi W, Elsukova A, Le HT, et al. Organic ice resists. Nano Lett 2017;17:7886–91.
[19] Elsukova A, Han A, Zhao D, et al. Effect of molecular weight on the feature size in organic ice resists. Nano Lett 2018;18:7576–82.
[20] Hong Y, Zhao D, Liu D, et al. Three-dimensional in situ electron-beam lithography using water ice. Nano Lett 2018;18:5036–41.
[21] Tiddi W, Elsukova A, Beleggia M, et al. Organic ice resists for 3D electron-beam processing: instrumentation and operation. Microelectron Eng 2018;192:38–43.
[22] Tiddi W. Organic ice resists for electron-beam lithography: instrumentation and processes. Ph.D. Thesis, Technical University of Denmark, 2018.
[23] Yasin S, Hasko DG, Ahmed H. Comparison of MIBK/IPA and water/IPA as PMMA developers for electron beam nanolithography. Microelectron Eng 2002;61–62:745–53.
[24] Namatsu H, Yamaguchi T, Nagase M, et al. Nano-patterning of a hydrogen silsesquioxane resist with reduced linewidth fluctuations. Microelectron Eng 1998;41–42:331–4.
[25] Hari S, Hagen CW, Verduin T, et al. Size and shape control of sub-20 nm patterns fabricated using focused electron beam-induced processing. J Micro/Nanolithogr, MEMS, MOEMS 2014;13.
[26] Aieta F, Genevet P, Kats M, et al. Aberrations of flat lenses and aplanatic metasurfaces. Opt Express 2013;21:31530.
[27] Kostovski G, Stoddart PR, Mitchell A. The optical fiber tip: An inherently light-coupled microscopic platform for micro- and nanotechnologies. Adv Mater 2014;26:3798–820.
[28] Sirringhaus H, Kawase T, Friend RH, et al. High-resolution inkjet printing of all-polymer transistor circuits. Science 2000;290:2123–6.
[29] Melchels FPW, Feijen J, Grijpma DW. A review on stereolithography and its applications in biomedical engineering. Biomaterials 2010;31:6121–30.
[30] Kawata S, Sun H-B, Tanaka T, et al. Finer features for functional microdevices. Nature 2001;412:697–8.
[31] Han A, Chervinsky J, Branton D, et al. An ice lithography instrument. Rev Sci Instrum 2011;82.
[32] Shawrav MM, Taus P, Wanzenboeck HD, et al. Highly conductive and pure gold nanostructures grown by electron beam induced deposition. Sci Rep 2016;6:34003.
[33] Sengupta S, Li C, Baumier C, et al. Superconducting nanowires by electron-beam-induced deposition. Appl Phys Lett 2015;106:042601.

[34] Bresin M, Botman A, Randolph SJ, et al. Liquid phase electron-beam-induced deposition on bulk substrates using environmental scanning electron microscopy. Microsc Microanal 2014;20:376–84.
[35] Bahlke ME, Mendoza HA, Ashall DT, et al. Dry lithography of large-area, thin-film organic semiconductors using frozen CO_2 resists. Adv Mater 2012;24:6136–40.
[36] Wieland MJ, Derks H, Gupta H, et al. Throughput enhancement technique for MAPPER maskless lithography. Proc SPIE 2010;7637:76371Z.

Ding Zhao received his Ph.D. degree in Optical Engineering from Zhejiang University, China in 2016. He was a postdoctoral researcher at Zhejiang University from 2016 to 2018. Currently, he is a H.C. Ørsted Postdoctoral Fellow at Technical University of Denmark. His research interests focus on advanced nanolithography and nanopatterning methods.

Min Qiu received the Ph.D. degree in Physics from Zhejiang University, China in 1999. He became an assistant professor and a full professor at the Royal Institute of Technology (KTH), Sweden, in 2001 and 2009, respectively. Since 2010, he worked as a professor at Zhejiang University. He was the Director of State Key Laboratory of Modern Optical Instrumentation, Zhejiang University. In 2018 he joined Westlake University as a Chair Professor of Photonics and Vice President for Research. His research interests include nanofabrication technology, nanophotonics, and green photonics.